Proceedings of the 12th International Conference on
Aluminium Alloys, September 5-9, 2010, Yokohama, Japan

pp. 1273-1278

Nucleation and Growth Dynamics of the α-Al / β-Al_5FeSi Eutectic in a Complex Al-Si-Cu-Fe Alloy

Sofiane Terzi[1], John A. Taylor[2], Young-Hee Cho[1], Luc Salvo[3], Michel Suéry[3], Elodie Boller[4], Arne K. Dahle[1]

[1]ARC CoE for Design in Light Metals, Materials Engineering, The University of Queensland, Brisbane QLD 4072, Australia

[2] CAST CRC, UDP No. 055, The University of Queensland, Brisbane QLD 4072, Australia

[3] Université de Grenoble, SIMaP/GPM2, UMR CNRS 5266, BP 46, 38402 Saint-Martin d'Hères Cedex, France

[4] ESRF, 156 rue des Martyrs, BP 220, 38043 Grenoble Cedex 9, France

Secondary-sourced recycled aluminium alloys can exhibit high levels of different impurities. It is well known that the presence of iron, the most common impurity, can lead to the formation of hard and brittle intermetallic phases which are detrimental to the machining properties and the mechanical behaviour of the material in service. The purpose of this work is to study the nucleation and growth of the β-Al_5FeSi intermetallic phase in the framework of the eutectic reaction: Liquid → α-Al + β-Al_5FeSi. In situ X-ray microtomography has been used to investigate the formation of the irregular eutectic β-phase plates during the solidification at low cooling rate of an Al-8Si-4Cu-0.8Fe alloy. The results show that only a few plates form, nucleating early near the sample surface. Next, growth occurs very rapidly in the principal growth direction and slowly in the thickness direction. The plates are highly branched and appear to form as a divorced eutectic, i.e. not coupled with the α-Al. These features are inconsistent with the common irregular eutectic solidification theory based on the Jackson and Hunt model.

Keywords: *X-ray microtomography; Fe-containing intermetallics; Aluminum alloys; Solidification microstructure; Eutectic solidification.*

1. Introduction

In commercial aluminium alloys, iron is a common impurity and can lead to the formation of hard and brittle β-Al_5FeSi intermetallic particles generally via a binary eutectic reaction (Liq. → α-Al + β-Al_5FeSi) at moderate Fe contents [1]. The β-Al_5FeSi phase (referred to as β phase throughout) is a highly faceted phase which forms as an irregular eutectic together with α-Al. While regular eutectic growth is the subject of a properly constructed theory, the formation of irregular eutectics is poorly understood. Only a few models describing the growth of irregular eutectics are presented in the literature [2,3]. These are all largely extensions of the Jackson and Hunt theory [4] describing regular eutectic growth. The aim of this work is to shed light on the formation of the β phase in the context of a better understanding of solidification of irregular eutectics. For this purpose, synchrotron X-ray in situ tomography has been used to observe in 3-D and real-time the solidification at low cooling rate of an Al-Si-Cu-Fe alloy.

2. Experimental Procedure

An Al-8%Si-4%Cu-0.8%Fe[1] alloy was prepared by mixing aluminium (99.94% purity), Si metal (99.5% purity), copper (electrical-grade Cu bar) and a commercial Fe-20%Al master alloy. A small 1.5 mm diameter cylindrical specimen was machined from the casting and used in the synchrotron in situ solidification experiment. The experimental set-up for the in situ microtomography is similar to

[1] All alloy compositions in this paper are expressed in weight %.

that used in previous work [5,6]. The sample was heated at 20ºC min^{-1} to a temperature of 620ºC and held isothermally for 5 min to ensure complete melting. It was then cooled down at 1.4ºC min^{-1} until complete solidification had occurred. Throughout the experiment, the specimen is supported by its own oxide skin and thus remains close to its original shape.

Microtomographic imaging was performed throughout the whole cooling process. 600 X-ray projections were taken during each 180º rotation of the sample. The scan time to complete the 600 projections is about 36 s and the total time for each full 180º scan and return to original position is about 57 s. The voxel size was set to $(1.4\ \mu m)^3$, and 1024^3 voxels of data is then gathered in each full scan to image the whole sample. Classical image corrections involving dark field images, flat field images and a ring-artefact correction algorithm were applied before the final 3-D reconstruction [7]. After reconstruction, in order to perform calculations with a conventional computer, a voxel binning technique has been applied to reduce the image size from 1024^3 to 512^3 voxels whenever calculations were performed on the whole volume. Otherwise, crops were made on the full resolution images in order to analyse particular regions of interest in greater detail. A noise reduction treatment (3-D median filter) was then applied to the raw images and a combination of thresholding, erosion, dilation and a 3-D region growing algorithm were used to distinguish the β phase plates from the rest of the sample. *ImageJ* software was used for these image treatments while the 3-D measurements and visualisations were performed with *Amira*® software.

3. Results and Discussion

The first reaction observed during solidification of the alloy (at about 595ºC) is the formation and growth of the primary α-Al dendrites, appearing slightly darker than the liquid. The second reaction is the nucleation and growth of the β-Al_5FeSi phase, which appears very bright due to its high content of highly absorbent Fe atoms. This phase starts to nucleate at 584ºC and its growth is largely completed by 557ºC. At about 569ºC the formation of the Al-Si eutectic in then observed. The acicular silicon phase appears in dark contrast in the tomography images. Fig. 1 shows these different phases coexisting at 555ºC. Once a temperature of 518ºC is reached, the remaining liquid then starts to transform into the complex eutectic containing the Al_2Cu phase. Despite slight variations in temperature values, the temperatures of these key reactions are consistent with the literature [8] and the predictions from the *Thermo-Calc*® software.

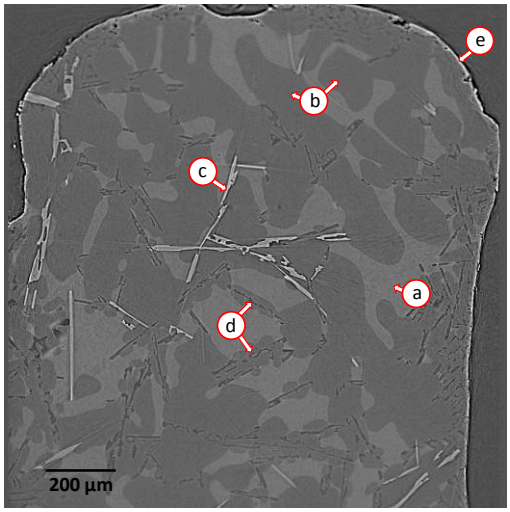

Fig. 1. Vertical slice extracted from the 3-D reconstructed X-ray tomography volume showing the different phases observed at t_0 + 45.6 min (555ºC): (a) liquid, (b) α-Al dendrite, (c) β-Al_5FeSi plate, (d) Al-Si eutectic and (e) outer oxide skin.

3.1 Nucleation of the β phase

Analysis of microtomography data has shown that only four independent β phase nucleation events occurred in the whole reconstructed volume (~ 2 mm^3) during the pre-Al-Si eutectic period.

The observed nucleation rate is lower than that suggested by Lee *et al.* [9,10] in a post-mortem tomography study performed on a similar alloy. This result may be associated with the much higher cooling rate in their work (20ºC min^{-1}) compared with 1.4ºC min^{-1} in the current work. However, as in the present study, some plates which nucleated outside the reconstructed region can grow into the imaged volume and become partially observable later. By performing a post-mortem analysis it is not possible to distinguish the plates that have nucleated outside the considered volume and therefore the nucleation rate appears higher than it actually is. During the solidification process, the complexity of the microstructure continually increases as the volume and the number of solid phases increases. It should also be noted that additional β nucleation events may have occurred later during the Al-Si eutectic growth period, in a ternary eutectic reaction. In a few cases it is hard to distinguish, without ambiguity, between a new nucleation occurring from the outer oxide and a branching event from a previously existing β plate. These cases involve a very small fraction of the total volume of β phase and are not discussed further in this paper.

It was observed that the four β phase nucleation events, which occurred before the formation of Al-Si eutectic, are all initiated at the surface of the sample. Fig. **2** shows the 3-D sequence of the nucleation and growth of these β plates. The first nucleation occurs at t_0 + 24.7 min and the three others plates appear simultaneously at t_0 + 27.6 min (Fig. **2**a).

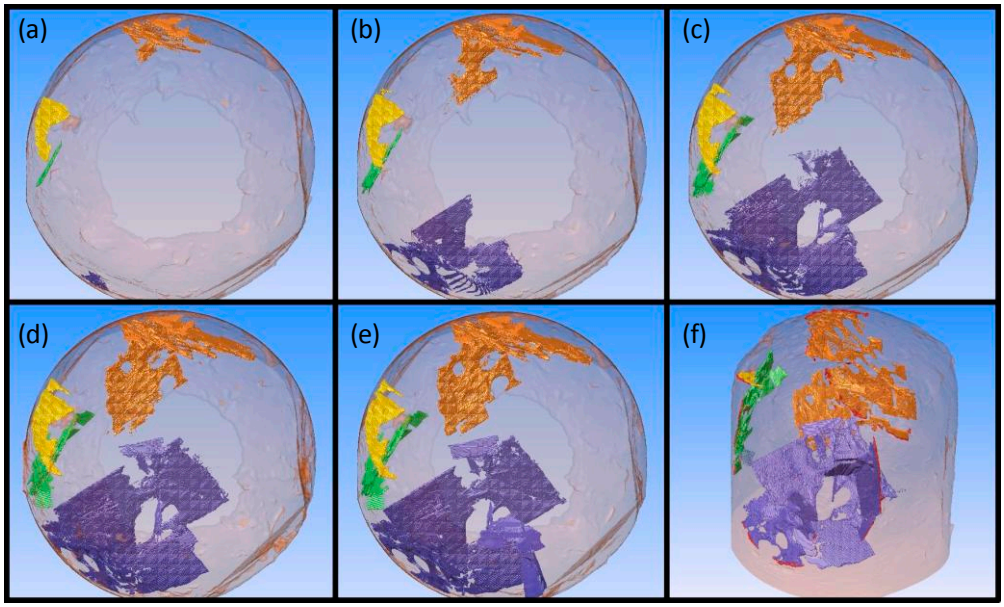

Fig. 2. Sequence of fully reconstructed sample volumes showing the four surface-nucleated β plates at several time steps. The top-down images (a) to (e) correspond to the time steps (a) t_0 + 27.6 min, (b) t_0 + 28.5 min, (c) t_0 + 29.5 min, (d) t_0 + 30.4 min, (e) t_0 + 32.3 min and the oblique view image to the time step (f) t_0 + 32.3 min.

As the plates grow, the β phase, which was previously confined to the periphery of the sample, reaches the centre of the sample (Fig. **2**e-f). During the cooling process, the increasing volume of aluminium dendrites combined with the volumetric shrinkage of the sample leads to increasing contact and interaction between the plates, branches and dendrites. The β plates can then become detached from their original nucleation site. Consequently, once the sample is fully solidified, some plates may appear disconnected from other plates or to the outer boundary. A post-mortem observation can therefore give the impression that these plates were nucleated in the bulk of the sample. In the present study, detailed examination of the plate evolution, in each case where this occurred, revealed an original contact point with another β plate or with the outer oxide skin.

Several authors have suggested that aluminium oxide can be a nucleant for the β phase [11-13]. The observation that all nucleation occurred on the outer oxide skin of the sample is in agreement with this idea. However, in the literature, two principal mechanisms have been proposed for nucleation of β phase: (i) nucleation on small entrained oxide films called "bifilms" within the melt thus yielding centreline cracks observed in many β plates [11-13], and (ii) nucleation on AlP particles [14-16]. Clearly neither occurred in this study and no nucleation of β phase occurred in the bulk liquid. Nevertheless, this should not be taken as evidence against either mechanism, since neither was varied in a controlled manner in our work. This would be an interesting topic for future study.

Observation has also shown that the nucleation of β phase is uncoupled with the nucleation of eutectic α-Al. The formation of β plates can be observed without the presence of any eutectic α-Al near the β nucleation site. It is suspected that the β phase is not a good nucleant for the α-Al phase. This point will be discussed further in the following paragraph.

3.2 Growth of β plates

In the literature, solid phases of irregular eutectic (formed in the framework of the reaction Liq. → $Solid_1$+$Solid_2$) are assumed to nucleate and grow in a coupled way [2,3]. In the present study, the nucleation and growth of the β phase is not systematically coupled with the nucleation and growth of the eutectic α-Al phase. Fig. 3a-b shows the appearance of two β plates nucleated at the surface of the sample. It is clear that no α-Al phase has nucleated from the nucleation point during the growth of the β plates. These observations are substantiated by the presence of dendrite imprints on the surface of the β phase visible in high resolution 3-D images of plates (Fig. 4). Indeed, if the eutectic α-Al had formed on the surfaces of the β plate it would have been impossible for such morphologies to form. The α-Al / β-Al_5FeSi eutectic appears to be weakly coupled and closer to a divorced eutectic with separate formation of the two eutectic phases. Models based on the Jackson and Hunt approach are therefore unable to adequately describe the formation of the α-Al / β-Al_5FeSi irregular eutectic.

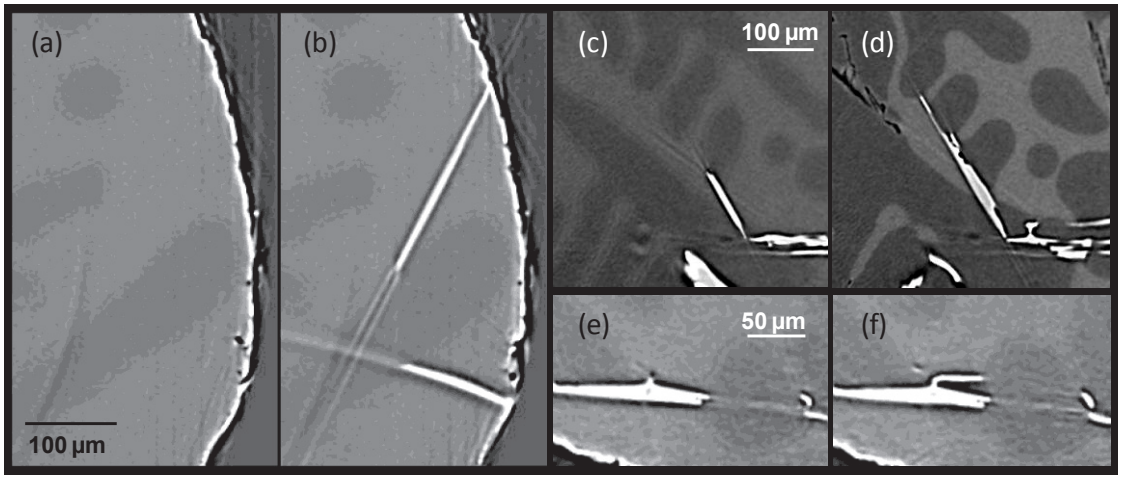

Fig. 3. 2-D images extracted from the 3-D reconstructed volume. Independent nucleation of β plates from the outer oxide skin is shown in (a) t_0 + 26.6 min and (b) t_0 + 27.6 min; interrupted and erratic β plate growth in (c) t_0 + 31.3 min and (d) t_0 + 39.9 min; and quasi-parallel branching in (e) t_0 + 28.5 min and (f) t_0 + 29.5 min. Note: the dark rims surrounding the bright β plate are imaging artefacts not aluminium phase.

As the β phase forms in a eutectic reaction (Liq. → α-Al + β-Al_5FeSi) it is accompanied by the α-Al phase. Our results strongly suggest that the α-Al eutectic phase grows on pre-existing α-Al dendrites rather than re-nucleating on or near the β plate. This can occur in two different forms: (i) uncoupled, the α-Al grows on an existing dendrite that is physically separated from the plate, and (ii)

coupled, the eutectic α-Al can grow on the surface of a β plate through impingement when the plate comes into direct contact with pre-existing α-Al dendrites.

Observations have shown that β plates grow very rapidly in the lateral direction. Once nucleated, a plate (or a branch) grows until it impinges on a dendrite, the outer boundary, or another β plate. At each time step, it was observed that β plates and branches have at least one other contact point other than the original nucleation site. This suggests that the time elapsed to reach an obstacle from the nucleation site is inferior to the time resolution. The maximum distance observed between a nucleation site and an impingement point is about 710 μm. This indicates that the growth rate can be greater than ~750 μm min^{-1}. This result is in agreement with a recent in situ 2-D experiment performed at higher cooling rate from Wang *et al.* [10] who reported a maximum growth of 100 μm s^{-1}.

During fast lateral growth episodes, the thickness of plates is very small thus allowing a very efficient sideways solute rejection at the tip of the plate. Once impingement occurs, an increase in the β plate thickness (estimated to be ~2 μm min^{-1}) is observed in most cases. This thickening is central to two important mechanisms: (i) the apparent erratic growth of the β plates, and (ii) the quasi-parallel branching. After impingement, the thickness increases such that plate growth follows the surface of the dendrite at a growth rate dependent on the angle between the dendrite surface and the plane of the plate. Once past the obstacle, the plates can then grow quickly again by lateral growth until the next impingement. This mechanism shown in Fig. 3c-d, appears to explain the very erratic behaviour of plate growth. As previously mentioned, the eutectic α-Al can grow from an impingement point, meaning a layer can then be formed on the surface of β plates. This can lead to a blockage of the lateral growth and can stop the thickening locally while still allowing the thickness to increase at some other points. Once the jog extends past the obstruction the plate becomes free to again grow laterally in its original preferred orientation (Fig. 3c-d).

3.3 Branching

No parallel branching of plates is observed. This feature is clearly visible in Fig. 4. Considering the complex 3-D structure of plates, it is difficult to measure an average lamellar spacing, such as is proposed and required in 2-D models for irregular eutectics [2,3]. Furthermore, we have observed that plates which appear isolated in 2-D section are usually interconnected in 3-D and originate from the

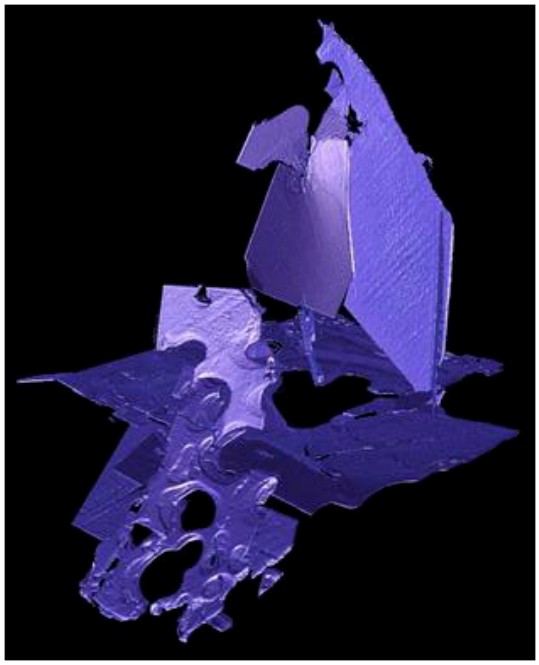

Fig. 4. Full resolution and advanced rendering 3-D image of a β plate at t_0 + 32.3 min (T = 573 ºC). Note the complex branching of the plate and the dendrite arm impressions and evidence of by-passing.

same nucleation event. This confirms that 2-D models presented in the literature are not appropriate for the irregular α-Al / β-Al_5FeSi eutectic.

A high incidence of microtwinning on the (001) plane of β phase has been reported in literature [17,18]. In the present study, a wide range of values of branching angles have been measured. It is possible that some may correspond to twinning events. However, this mechanism alone cannot explain the complex branching obtained. Moreover, it has been shown that twin planes are parallel to the growth direction which reduces the branching possibility during simple growth in the liquid phase [17]. We propose that a physical interaction with objects (particularly contacting dendrites) is needed in most cases to allow β plate branching. Small movements of the outer oxide boundary and of dendrites during shrinkage of the sample appears to be sufficient to deform, bend, or even fracture thin parts of plates which can then provide free space for continued growth. This mechanism involves quick deformation which is difficult to resolve in the time-steps of our experiments. However, this theory is supported by observation of deformation of plates due to internal contact and by the fact that branched β plates always appear to grow at angles dictated in part by the dendrite arm impinging at the branching point, rather than any fixed, predisposed angular relationship.

Acknowledgements

This work was carried out in the framework of the project ANR-05-BLAN-0286-01 "TOMOSOLIDAL" supported by the "French Agence Nationale de la Recherche", which is gratefully acknowledged. The authors wish to thank all staff members of the ID19 beam line of ESRF Grenoble for their technical support. AKD wishes to thank the Australian Academy of Science for the Bede Morris Fellowship enabling his travel to Grenoble.

References

[1] J.A. Taylor, G.B. Schaffer, and D.H. StJohn: Met. Mat. Trans. A 30 (1999) 1651-1655.
[2] E. Guzik, and D. Kopycinski: Met. Mat. Trans. A 37 (2006) 3057-3067.
[3] P. Magnin, and R. Trivedi: Acta Metallurgica Et Materialia 39 (1991) 453-467.
[4] K.A. Jackson, and J.D. Hunt: Trans. Metall. Soc. AIME 236 (1966) 1129-1142.
[5] S. Terzi, L. Salvo, M. Suéry, and E. Boller: Scripta Mat. 60 (2009) 671-674.
[6] S. Terzi, L. Salvo, M. Suery, A.K. Dahle, and E. Boller: Acta Mat. 58 (2010) 20-30.
[7] O. Ludwig, M. Dimichiel, L. Salvo, M. Suéry, and P. Falus: Met. Mat. Trans. A 36 (2005) 1515-1523.
[8] L. Backerüd, G. Chai, and J. Tamminen: *Solidification characteristics of aluminum alloys: Vol. 2 - foundry alloys*, (AFS/Skanaluminium, USA, 1990).
[9] P.D. Lee, J. Wang, and M. Li: *Modeling of Casting, Welding and Advanced Solidification Processes - XII* (Cruise - Vancouver to Alaska, 2009) pp 87-99.
[10] J. Wang, P.D. Lee, R.W. Hamilton, M. Li, and J. Allison: Scripta Mat. 60 (2008) 516-519.
[11] J. Campbell: Inter. J. of Metalcasting 3 (2009) 65-67.
[12] D.N. Miller, L. Lu, and A.K. Dahle: Met. Mat. Trans. B 37 (2006) 873-878.
[13] L. Narayanan, F. Samuel, and J. Gruzleski: Met. Mat. Trans. A 25 (1994) 1761-1773.
[14] Y.H. Cho, H.C. Lee, K.H. Oh, and A.K. Dahle: Met. Mat. Trans. A 39 (2008) 2435-2448.
[15] G. Sigworth: Inter. J. of Metalcasting 3 (2009) 68-70.
[16] L. Lu, and A.K. Dahle: Met. Mat. Trans. A 36 (2005) 819-835.
[17] M.H. Mulazimoglu, A. Zaluska, J.E. Gruzleski, and F. Paray: Met. Mat. Trans. A 27 (1996) 929-936.
[18] V. Hansen, B. Hauback, M. Sundberg, C. Rømming, and J. Gjønnes: Acta Cryst. B 54 (1998) 351-357.